JOURNAL OF THE PHYSICAL SOCIETY OF JAPAN, Vol. 47, No. 5, NOVEMBER, 1979

Electronic Properties of a Semiconductor Superlattice. I. Self-Consistent Calculation of Subband Structure and Optical Spectra

Tsuneya ANDO and Shojiro MORI†

Institute of Applied Physics, University of Tsukuba, Sakura, Ibaraki 300-31
†*Department of Physics, University of Tokyo, 7-3-1, Hongo, Bunkyo-ku, Tokyo 113*

(Received June 13, 1979)

The subband structure of a heavily doped *n*-type GaAs–$Ga_{1-x}Al_xAs$ superlattice is calculated. A band bending effect caused by charge transfer from the $Ga_{1-x}Al_xAs$ to GaAs layers is taken into account self-consistently in the Hartree approximation. When the wavefunction along the superlattice direction is rather localized, the band bending effect is crucial especially in the case of modulation doping where only the $Ga_{1-x}Al_xAs$ layer is heavily doped and the GaAs layer remains undoped. Calculated results are in good agreement with recent experiments. Many-body effects such as exchange and correlation are studied in the density-functional formulation, but shown to be unimportant. Intersubband optical absorptions are also investigated. A local field effect can shift resonance energies to higher energy side considerably.

§1. Introduction

The evolution of molecular-beam epitaxy has allowed access to man-made semiconductor superlattices, which consist of periodic heterostructures of alternating, ultrathin layers of two semiconductors that closely match in lattice constant. Heterostructures made of GaAs and $Ga_{1-x}Al_xAs$ have been studied extensively. In case of sufficiently thick $Ga_{1-x}Al_xAs$, electrons are bounded in single potential wells of GaAs. With the decrease of the thickness couplings between adjacent wells become important and eventually cause the superlattice formation. As a result of extensive experimental study of various properties such as electron tunneling,[1,2] transport[3,4] interband optical absorptions,[5-8] and Raman scatterings,[9,10] it has been known that the boundary is sharp to within a lattice constant and that a simple model of a square well potential works quite well. Further, the parameters of the potential are now well-established. Correspondingly, previous theoretical calculations on the subband structure and related quantities have been done in the simple Kronig-Penney model.

Recently Dingle *et al.* used a modulation doping technique to achieve heavily doped superlattices having high mobilities.[11,12] In this technique only the $Ga_{1-x}Al_xAs$ layers are doped and the GaAs layers where electrons mainly exist remain undoped. In such heavily doped cases a band bending effect neglected completely in previous calculations becomes appreciable, and we must calculate the subband structure self-consistently including effects of charge transfer from the $Ga_{1-x}Al_xAs$ to GaAs layers. Charge transfer effects in layer compounds like graphite intercalations have been attracting much attention.[13] The present superlattice problem can be regarded as the simplest example.

The purpose of the present series of papers is to study electronic properties of heavily doped GaAs–$Ga_{1-x}Al_xAs$ superlattices. In this paper we present results of the calculation of the subband structure and demonstrate the importance of the self-consistency. We employ the Kronig-Penney model characterized by a single effective mass and a barrier height for the lattice potential and take into account the charge transfer effect by including the potential of ionized donors and that of electrons themselves in the Hartree approximation. A density-functional formulation is employed to see effects of exchange and correlation. We calculate also optical absorption spectra, and show importance of a local field effect, i.e. that absorption

peaks can be shifted from subband energy separations considerably.

In §2 a brief discussion is made on the model, approximations, and the method of calculations. A dynamical conductivity which describes the optical absorption is introduced. Examples of results are presented and compared with experiments in §3. A summary and a conclusion are given in §4.

§2. Subband Structure and Optical Absorption

2.1 Subband structure

We replace the $Ga_{1-x}Al_xAs$ layer by a simple potential barrier with a height V_0. In the absence of doping the problem is reduced to the elementary Kronig-Penney model. When donors are introduced in the $Ga_{1-x}Al_xAs$ layer, they are ionized and produce electrons in the GaAs layer. Dingle *et al.* used Si as donors.[11] Binding energies of Si^+ ions are still uncertain but have been assumed to be sufficiently small.[11,12] As has been done in the inversion layer problem[14] we replace Si^+ ions by a positive uniform distribution in the $Ga_{1-x}Al_xAs$ layers. We use the similar model of a uniform charge distribution also in the case of uniform doping where donors are distributed equally in both layers. The neglect of discreteness of charge is not good if binding energies are sufficiently large and binding lengths are smaller than the thickness of the GaAs layer. In bulk GaAs, we have $E_B^* \sim 5$ meV and $a_B^* \sim 100$ A, where E_B^* and a_B^* are the binding energy and the effective Bohr radius, respectively, of a single isolated donor. These numbers are comparable to corresponding quantities appearing in the present calculation. However, we are dealing with rather high concentrations of electrons, i.e. typically $N_D \sim 10^{18}\,\mathrm{cm}^{-3}$, where N_D is the concentration of donors in a unit volume. In such a case overlapping and screening of potentials are sufficiently large and each ion has no bound state.[15] Therefore, we expect that the present model is reasonable as a starting approximation. In a forthcoming paper we shall study effects of discrete charges on the carrier mobility.

We choose the z direction as the superlattice direction. The wavefunction corresponding to the electron motion in the xy plane is given by a simple plane wave, and the wavefunction in the z direction satisfies

$$-\frac{\hbar^2}{2m}\frac{\mathrm{d}^2}{\mathrm{d}z^2}\zeta_{nk_z}(z)+V(z)\zeta_{nk_z}(z)=\varepsilon_n(k_z)\zeta_{nk_z}(z), \tag{2.1}$$

with m being the effective mass and

$$V(z)=\sum_{l=-\infty}^{+\infty} V_0\theta\left[\left(\frac{d_2}{2}\right)^2-\left(z-\left(l+\frac{1}{2}\right)d\right)^2\right]+v(z), \tag{2.2}$$

where $\theta(x)$ is the step function, d_1 is the thickness of the GaAs layer, d is the period of the superlattice ($d=d_1+d_2$ with d_2 being the thickness of the $Ga_{1-x}Al_xAs$ layer), and $v(z)$ is the potential of positive charges and electrons themselves. In the Hartree approximation we have

$$\frac{\mathrm{d}^2}{\mathrm{d}z^2}v(z)=-\frac{4\pi e^2}{\kappa}n(z)+\frac{4\pi e^2}{\kappa}N_D\frac{d}{d_2}\sum_{l=-\infty}^{+\infty}\theta\left[\left(\frac{d_2}{2}\right)^2-\left(z-\left(l+\frac{1}{2}\right)d\right)^2\right], \tag{2.3}$$

for the modulation doping (MD) case, where $n(z)$ is the electron density distribution and κ is the static dielectric constant. The dielectric constant of $Ga_{1-x}Al_xAs$ is not known and is assumed to be the same as that of GaAs. We have

$$N_D=n\equiv N_s/d, \tag{2.4}$$

with

$$N_s=\int_{-d/2}^{d/2}\mathrm{d}z\, n(z), \tag{2.5}$$

where N_s is the areal electron density per GaAs layer. In case of uniform doping (UD) the second term in the right hand side of eq. (2.3) should be replaced by $4\pi e^2 N_D/\kappa$.

To solve eq. (2.1) we expand the wavefunction as

$$\zeta_{nk_z}(z)=\exp(ik_z z)\sum_{l=-\infty}^{+\infty} c_l^{(n)}(k_z)\exp\left(i\frac{2\pi lz}{d}\right), \tag{2.6}$$

where

$$\sum_{l=-\infty}^{+\infty} c_l^{(n)}(k_z)^* c_l^{(n')}(k_z)=\delta_{nn'}. \tag{2.7}$$

We then get

$$\frac{\hbar^2}{2m}\left(k_z+\frac{2\pi l}{d}\right)^2 c_l^{(n)}(k_z)+\sum_{l'=-\infty}^{+\infty} V_{l-l'}c_{l'}^{(n)}(k_z)=\varepsilon_n(k_z)c_l^{(n)}(k_z), \tag{2.8}$$

with

$$V(z)=\sum_{l=-\infty}^{+\infty} V_l\exp\left(i\frac{2\pi l}{d}z\right). \tag{2.9}$$

The electron density distribution is given by

$$n(z)=2\sum_n\frac{1}{L^2}\sum_{\boldsymbol{k}}\theta\left[E_F-\varepsilon_n(k_z)-\frac{\hbar^2k^2}{2m}\right]|\zeta_{nk_z}(z)|^2, \tag{2.10}$$

where the factor 2 comes from the spin degeneracy, $\boldsymbol{k}=(k_x, k_y)$ is the component in the xy plane, and E_F is the Fermi energy determined by the charge neutrality condition (2.4). In terms of the Fourier transform of $n(z)$, i.e.

$$n(z)=\sum_{l=-\infty}^{+\infty} n_l\exp\left(i\frac{2\pi l}{d}z\right), \tag{2.11}$$

we have

$$V_l=-\frac{V_0}{\pi l}\sin\frac{\pi l d_1}{d}+\frac{4\pi e^2}{\kappa}\left(\frac{d}{2\pi l}\right)^2\left[n_l-N_D\frac{d}{d_2}\frac{(-1)^l}{\pi l}\sin\frac{\pi l d_2}{d}\right], \tag{2.12}$$

for $l\neq 0$ in the MD case. We choose the origin of energy as $V(z=d_1/2)=0$, which determines the value of $V_{l=0}$.

The Hartree approximation usually overestimates the Coulomb repulsive force of other electrons and sometimes many-body effects such as exchange and correlation become important. We study the exchange-correlation effect in the density-functional formulation. In this formulation, the effect is taken into account by introducing an exchange-correlation potential $v_{xc}[n(z)]$ which is given by a functional derivative of the exchange-correlation part of the ground state energy with respect to the electron density.[16-18] In the well-established local approximation v_{xc} becomes the exchange-correlation part of the chemical potential, μ_{xc}, of the uniform electron gas having the same local electron concentration. Strictly speaking, this potential can be used only for the calculation of the ground state energy and the electron density distribution. However, it can be used in a good approximation for the subband structure calculation also as has been discussed previously.[19] This exchange-correlation potential has been calculated by a number of people. We use here an expression parameterized by Gunnarson and Lundqvist.[20]

$$v_{xc}[n(z)]=-\frac{2}{\pi\alpha r_s}\left[1+0.0545\,r_s\ln\left(1+\frac{11.4}{r_s}\right)\right]\frac{me^4}{2\kappa^2\hbar^2}, \tag{2.13}$$

where $\alpha=(4/9\pi)^{1/3}=0.521$ and

$$n(z)=\left[\frac{4\pi}{3}(a_B^* r_s)^3\right]^{-1}, \tag{2.14}$$

with $a_B^*=\kappa\hbar^2/me^2$.

2.2 *Optical absorption*

Inter-subband transitions are induced by a far-infrared radiation polarized in the z direction. In single-layer cases like inversion layers on semiconductor surfaces, a resonance occurs when an

induced current becomes maximum at a fixed external electric field. The situation is different in the superlattice with infinitely many layers. Since the wavelength of light is much larger than the period of the superlattice, the system can be regarded as a medium having a macroscopic conductivity $\sigma_{zz}(\omega)$. According to conventional theory its poles give positions of optical absorptions. In single-layer cases resonance energies can be shifted from corresponding subband separations due to the depolarization effect.[21] Resonance energies can be shifted also in the superlattice. To illustrate this so-called local field effect, let us first consider an independent-layer model where each GaAs layer is sufficiently far from each other and can be treated as isolated. When an external electric field $De^{-i\omega t}$ is applied in the z direction, the induced current is given by

$$j(z)=\int dz'\sigma(z, z')E(z'), \tag{2.15}$$

where $\sigma(z, z')$ is the conductivity and $E(z)$ is the total electric field, which is related to the external field through

$$E(z)=D-\frac{4\pi i}{\omega\kappa}j(z), \tag{2.16}$$

in the limit of the infinite light velocity. Let us introduce a two-dimensional conductivity $\tilde{\sigma}_{2D}(\omega)$, defined by

$$d\bar{j}(\omega)=\int_{-d/2}^{d/2} dz\, j(z)=\tilde{\sigma}_{2D}(\omega)D. \tag{2.17}$$

We have the following relation between the macroscopic current $\bar{j}$ and electric field $\bar{E}$.

$$\bar{j}(\omega)=\frac{1}{d}\tilde{\sigma}_{2D}(\omega)D=\frac{1}{d}\tilde{\sigma}_{2D}(\omega)\left[1-\frac{4\pi i}{\omega\kappa}\frac{1}{d}\tilde{\sigma}_{2D}(\omega)\right]^{-1}\bar{E}. \tag{2.18}$$

In the independent-layer model, therefore, the macroscopic conductivity becomes

$$\sigma(\omega)=\frac{1}{d}\tilde{\sigma}_{2D}(\omega)\left[1-\frac{4\pi i}{\omega\kappa}\frac{1}{d}\tilde{\sigma}_{2D}(\omega)\right]^{-1}. \tag{2.19}$$

As has been shown in the case of semiconductor inversion layers, $\tilde{\sigma}_{2D}(\omega)$ is affected by the depolarization effect and its peak is shifted from subband separations by an amount of an effective plasmon frequency.[21] For simplicity, we consider the case that only the lowest subband is occupied by electrons and transitions to the first excited subband are dominant. We then have

$$\tilde{\sigma}_{2D}(\omega)=\sigma_{2D}(\omega)\left[1+\frac{4\pi i}{\omega\kappa}\frac{1}{\zeta}\sigma_{2D}(\omega)\right]^{-1}, \tag{2.20}$$

with ζ being of the order of the effective thickness of the GaAs layer and

$$\sigma_{2D}(\omega)=\frac{N_s e^2}{m}\frac{f_{10}(-i\omega)}{\omega_{10}^2-\omega^2-2i\omega/\tau}, \tag{2.21}$$

where $\hbar\omega_{10}=\varepsilon_1-\varepsilon_0$ is the energy separation, f_{10} is the oscillator strength, and τ is a phenomenological relaxation time. We get

$$\sigma(\omega)=\frac{N_s e^2 f_{10}(-i\omega)}{md}[\omega_{10}^2+\tilde{\omega}_p^2-\omega^2-2i\omega/\tau]^{-1}, \tag{2.22}$$

which shows that the resonance position is shifted to $(\omega_{10}^2+\tilde{\omega}_p^2)^{1/2}$ with

$$\tilde{\omega}_p^2=\frac{4\pi N_s e^2 f_{10}}{m\zeta}\left(1-\frac{\zeta}{d}\right). \tag{2.23}$$

In case of the square-well model with infinite barrier height, we have $\zeta\sim 0.58 d_1$. Thus the depo-

larization effect is not cancelled out except in the case that the wavefunction in the z direction is sufficiently extended and close to the plane wave. This is an example of the so-called local field effect.[22,23]

In actual superlattices, we expand the induced current, the electric field, and the conductivity as

$$j(z)=\sum j_l \exp\left(i\frac{2\pi lz}{d}\right), \tag{2.24}$$

$$E(z)=\sum E_l \exp\left(i\frac{2\pi lz}{d}\right), \tag{2.25}$$

and

$$\sigma(z, z')=\sum_l \sum_{l'} \sigma_{ll'}(\omega) \exp\left(i\frac{2\pi lz}{d}+i\frac{2\pi lz'}{d}\right). \tag{2.26}$$

Here we have

$$\sigma_{ll'}(\omega)=-i\frac{2}{L^3}\sum_n\sum_{n'}\sum_{k_z}\sum_k \frac{(nk_z|j_l|n'k_z)(n'k_z|j_{l'}|nk_z)}{\hbar\omega_{n'n}(k_z)} \times \frac{\theta\left[E_F-\varepsilon_n(k_z)-\dfrac{\hbar^2k^2}{2m}\right]-\theta\left[E_F-\varepsilon_{n'}(k_z)-\dfrac{\hbar^2k^2}{2m}\right]}{\omega_{n'n}(k_z)-\omega}, \tag{2.27}$$

with

$$(nk_z|j_l|n'k_z)=-\frac{\pi e\hbar}{md}\sum_{l'} c_{l'}^{(n)}(k_z)c_{l'+l}^{(n')}(k_z)\left[\frac{dk_z}{\pi}+2l'+l\right], \tag{2.28}$$

where $\hbar\omega_{n'n}(k_z)=\varepsilon_{n'}(k_z)-\varepsilon_n(k_z)$. In silicon inversion layers, a final state interaction called exciton-like effect is known to be important.[21] This is because the exchange and correlation effect is crucial in the inversion layer.[19] As will be shown in the next section, the many-body effect is not so important in our system. Therefore we neglect the exciton-like effect. We get

$$j_l=\sum \sigma_{ll'}E_{l'}, \tag{2.29}$$

and

$$E_l=D\delta_{l0}-\frac{4\pi i}{\omega\kappa}j_l, \tag{2.30}$$

which give

$$E_l=\left[1+\frac{4\pi i}{\omega\kappa}\hat{\sigma}(\omega)\right]^{-1}_{l0} D, \tag{2.31}$$

where $\hat{\sigma}(\omega)$ is a matrix whose components are given by $\sigma_{ll'}(\omega)$. The macroscopic current is given by

$$j(\omega)=j_{l=0}(\omega)=\left[\hat{\sigma}(\omega)\left[1+\frac{4\pi i}{\omega\kappa}\hat{\sigma}(\omega)\right]^{-1}\right]_{00} D, \tag{2.32}$$

and the macroscopic conductivity becomes

$$\sigma(\omega)=j(\omega)/E_{l=0}=\left[\hat{\sigma}(\omega)\left[1+\frac{4\pi i}{\omega\kappa}\hat{\sigma}(\omega)\right]^{-1}\right]_{00}\left[\left[1+\frac{4\pi i}{\omega\kappa}\hat{\sigma}(\omega)\right]^{-1}_{00}\right]^{-1}. \tag{2.33}$$

§3. Numerical Results and Comparison with Experiments

In numerical calculations we divide k_z into discrete points and truncate the summation over l' in eq. (2.8) at $l'=l_{max}$. The resulting matrix Hamiltonian is then diagonalized numerically. We can calculate the density distribution of electrons and the self-consistency is established iteratively by using the uniform electron distribution as an initial solution. We use $m=0.068m_0$, with m_0 being the free electron mass, $\kappa=11.9$, and $l_{max}=20$ which gives a convergent result in the case considered below.

An example of the density distribution, potential energies, and energy spectra calculated in the Hartree approximation is given in Fig. 1. We have assumed that $d_1 = 221$ A, $d_2 = 218$ A, $V_0 = 300$ meV, $N_D = 0.697 \times 10^{18} \text{cm}^{-3}$, and $N_s = 3.06 \times 10^{12} \text{cm}^{-2}$. For these parameters couplings between adjacent layers are weak for electrons in the three lowest subbands. The corresponding result in the simple Kronig-Penney model is given in Fig. 2. The importance of the band bending is readily seen. The increase and decrease of the potential energy at $z = 0$ and $z = d/2$, respectively, are very large and electrons are pushed toward the interface strongly if we include the band bending. Consequently, the electron density at $z = 0$ is only 1/3 of the peak value, and the lowest and next lowest subbands are already close to bonding and antibonding levels of the ground subbands associated with the two sub-layers which are separated by a potential barrier around $z = 0$.

An example in the UD case corresponding to Figs. 1 and 2 is shown in Fig. 3. The band bending is about a half of that in the MD case. The electron density at $z = 0$ is comparable to the peak value. Quantitatively. however, the band bending is still appreciable when the wavefunction is localized and the electron concentration is sufficiently large.

A result calculated in the density-functional

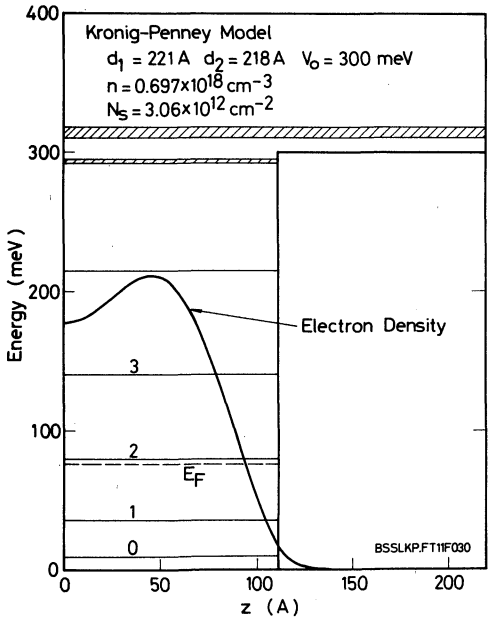

Fig. 2. An example of energy levels, density distribution of electrons, and the self-consistent potential in the Kronig-Penney model. The parameters are the same as in Fig. 1.

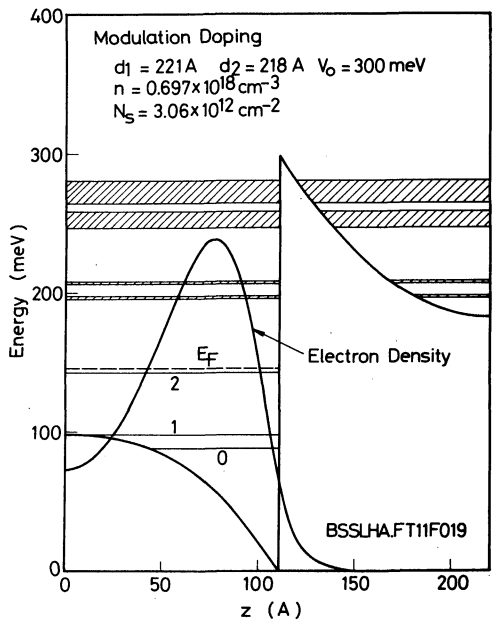

Fig. 1. An example of energy levels, density distribution of electrons, and the self-consistent potential in the modulation doping case calculated in the Hartree approximation. The subband widths are described by hatches.

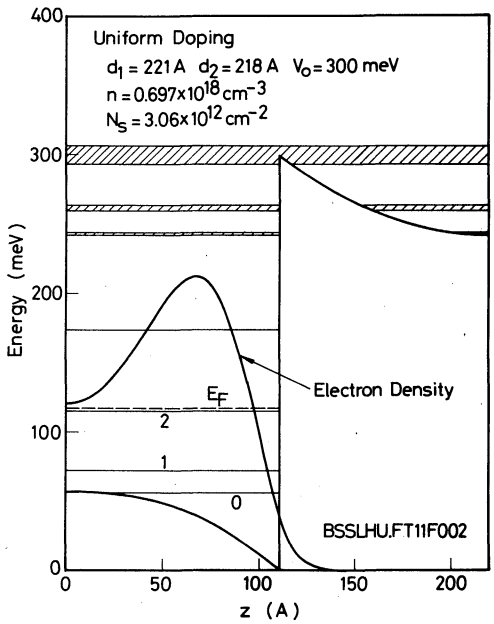

Fig. 3. An example of energy levels, density distribution of electrons, and self-consistent potential in the uniform doping case. The parameters are the same as in Fig. 1.

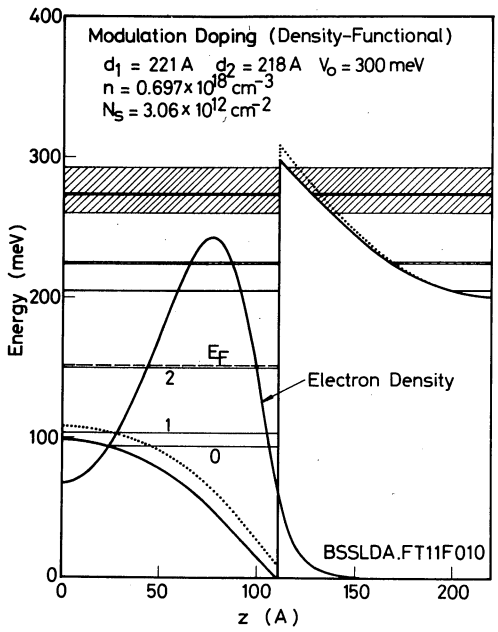

Fig. 4. An example of energy levels, density distribution of electrons, and self-consistent potential in the modulation doping case calculated in the density-functional formulation. The Hartree part of the potential is represented by a dotted line. Electrons are slightly pushed toward the interface, but the exchange-correlation effect is not so important.

formulation for the MD case is given in Fig. 4. The dotted line represents the Hartree part of the potential. The exchange and correlation slightly reduce the Coulomb repulsive force and electrons are further pushed toward the interface. However, they are not so important as in inversion and accumulation layers on Si.[23] This is because the effective mass of electrons is much smaller than in Si and the effective electron concentration is sufficiently large in GaAs.

Figure 5 shows calculated energies as a function of the electron concentration. We assumed the MD case with $d_1=d_2=200$ A, $V_0=300$ meV, and used the Hartree approximation. The Fermi energy, E_F, and the potential energies at $z=0$ and $z=d/2$ are also included. The potential energy at $z=d/2$ decreases almost linearly with N_s, i.e. with N_D, since $V(z=d/2)=V_0-2\pi e^2 N_s d/\kappa$ if we neglect the slight density of electrons in the $Ga_{1-x}Al_xAs$ layer. The Fermi level touches the bottom of the first excited subband around $N_s\sim 0.8\times 10^{12}$ cm^{-2} and that of the second excited subband around $N_s\sim 3.3\times 10^{12}$ cm^{-2}. Because of the band bending the energy of levels bounded in the GaAs layer increases with N_s. Around the electron concentration where they cross the $V(z=d/2)$ line, widths of the subbands increase drastically and their characters turn into three-dimensional rather two-dimensional. The levels with higher energies corresponding to extended states even for $N_s=0$ decrease in energy with N_s also because of the band bending. We can see interactions of these two different levels when they cross. Above $N_s\sim 4\times 10^{12}$ cm^{-2} the electron density distribution becomes extended and begins to have a considerable amount in the $Ga_{1-x}Al_xAs$ layer. This corresponds to the case of a partial charge transfer from the $Ga_{1-x}Al_x$ As layers.

Available experimental results are quite limited so far. Störmer *et al.* measured the Shubnikov-de Haas oscillation of the conductivity along the xy plane in samples corresponding to Figs. 1 and 4. They observed two periods which are very close to each other and obtained the energy separation of the two lowest subbands as 8.6 meV. The present calculation shown in Fig. 4 gives 9.4 meV in excellent agreement with their experiments. We should notice that it is given by 26.7 meV if we neglect the band bending effect. Thus we can conclude that the self-consistent calculation is crucial in this system and that its proper inclusion gives results which are in good agreement with the experiments. The present calculation shows that electrons occupy also the second excited subband. This does not contradict the experiments, however, since the number of those electrons is extremely small and they do not contribute to the oscillation.

Similar experiments have been performed in UD systems by Chang *et al.*[3] An example of calculated level structure corresponding to the sample (C) of their paper is shown in Fig. 6. We have assumed that $d_1=d_2=90$ A, $V_0=100$ meV, $N_D=1.9\times 10^{18}$ cm^{-3}, and $N_s=3.43\times 10^{12}$ cm^{-2}. The band bending effect increases widths of the lowest and next lowest subbands. The Kronig-Penney model predicts that $\Delta\varepsilon_0=|\varepsilon_0(k_z=0)-\varepsilon_0(k_z=\pi/d)|=2.5$ meV and $\Delta\varepsilon_1=21.5$ meV, while the present calculation gives $\Delta\varepsilon_0=4.0$ meV and $\Delta\varepsilon_1=27.6$ meV. The energy separation between the lowest and next lowest subbands is reduced about 10% by the band bending. In this case the self-consistency is not so important. From the period of the

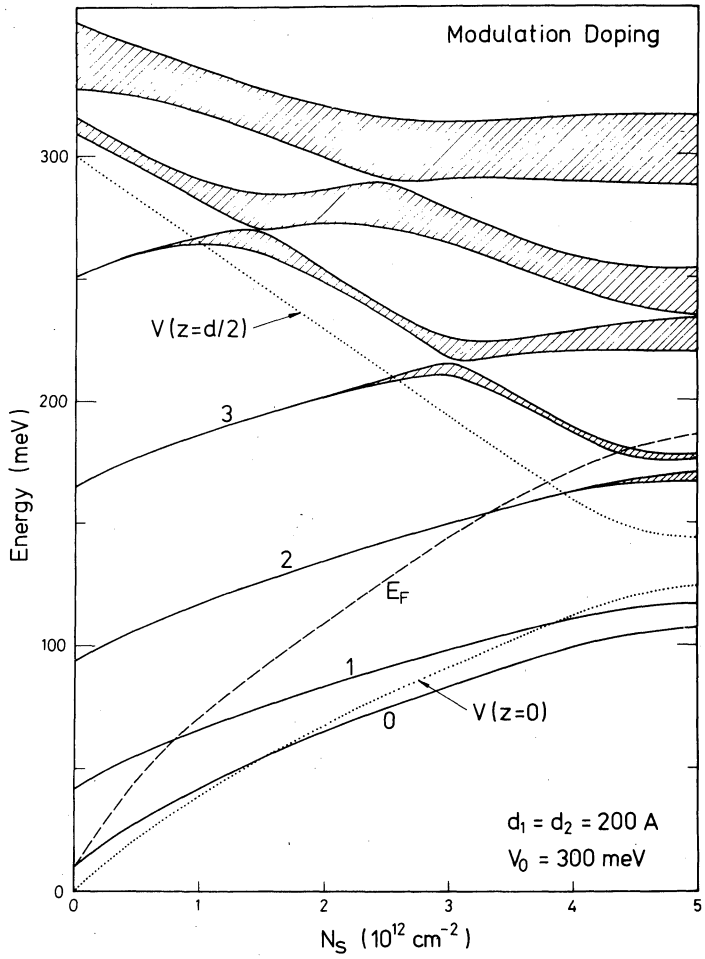

Fig. 5. Calculated energies as a function of the electron concentration in the modulation doping case. The subband widths are described by hatches.

Shubnikov-de Haas oscillation Chang *et al.* determined the Fermi energy measured from the lowest subband. The present calculation gives 89 meV which is in agreement with their experimental results given by 97 meV. The Kronig-Penney model gives 96 meV in better agreement. This is considered to be just a coincidence. We have calculated the subband structure by varying values of the various parameters slightly. The result shows that the Fermi energy measured from the bottom of the ground subband is rather insensitive to a slight change in the barrier height, but very sensitive to the electron concentration or the doping level. There might be an uncertainty in the measured value of N_D. Chang *et al.* determined it by low temperature Hall effect. Since electrons occupy two subbands which can have different mobilities, the Hall coefficient is not given by the total electron concentration. This problem will be discussed in a following paper. To make a more conclusive comparison, one should know more precise values of the doping level.

Direct information on the subband structure can, of course, be obtained by intersubband optical absorption. We have calculated the dynamical conductivity by truncating the summation over l' at $l'=l_{max}$ with $l_{max}=20$ in the case that $\hbar/\tau=5$ meV, $d_1=d_2=200$ A, and $V_0=300$ meV. Examples are shown in Fig. 7. We have taken into account only intersubband components and neglected the Drude type intrasubband contributions. The dotted lines represent $\sigma_{00}(\omega)$ which does not include the local field effect. Its peak positions are deter-

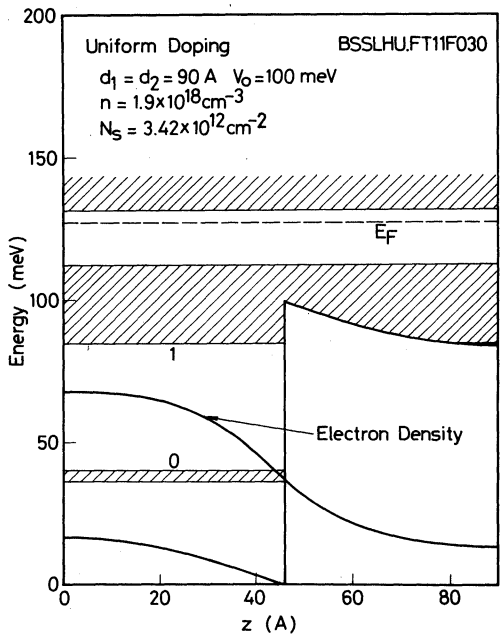

Fig. 6. Calculated energy levels, density distribution of electrons, and self-consistent potential in the uniform doping case. The thickness and barrier height are considerably smaller than in Figs. 1~4. The subband widths are described by hatches.

mined by the corresponding subband separations. The solid lines represent the macroscopic conductivity which contains the local field effect. The two low energy peaks for $N_s=1$, 2, and 3×10^{12} cm^{-2} arise from the transitions from $n=0$ to 1 and $n=1$ to 2. Consideration of the parity of states at $k_z=0$ gives a quasi-selection rule valid for low-lying subbands that transitions among states with even n and among those with odd n are almost forbidden. The amplitude of the 0 to 1 transition becomes smaller with the increase of N_s. This is partly because the electron occupation numbers of the subbands 0 and 1 become close to each other and the Pauli exclusion principle prohibits the transition. Further, the wavefunctions of the two subbands become similar to each other with the increase of the band bending. These two transitions correspond to those between the bands whose wavefunctions in the z direction are well localized. Therefore, the local field effect is very important and shifts the peak positions to higher energy side.

The transitions to the extended states, i.e. from $n=0$ to 3 and from $n=1$ to 4 appear around $\hbar\omega\sim150$ meV. The local field effect on these transitions is small as expected. At $N_s=4\times10^{12}$ cm^{-2} an additional absorption appears around $\hbar\omega\sim25$ meV. This arises from the transition to $n=3$ from $n=2$ which has become occupied by electrons. As can be seen in Fig. 5, the $n=2$ and 3 subbands have a

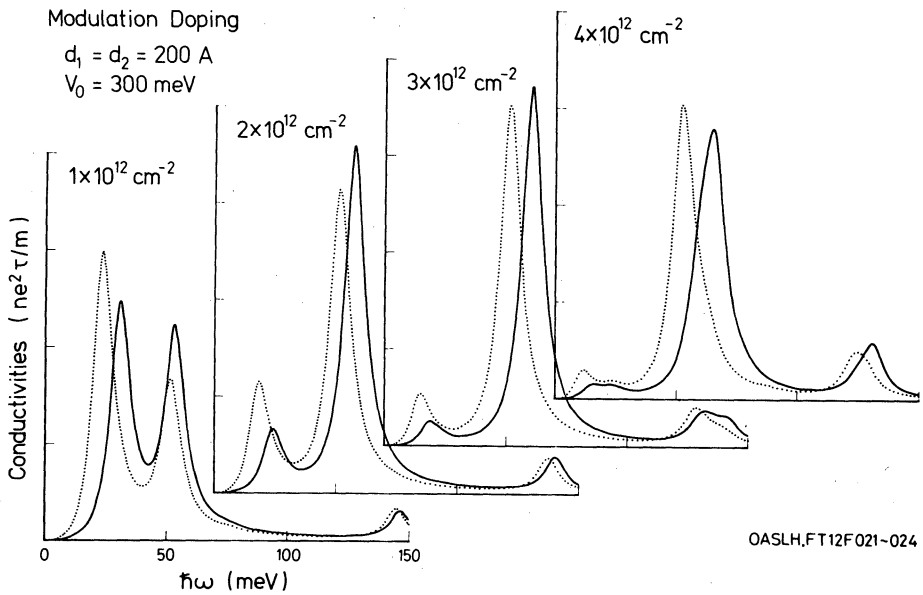

Fig. 7. Examples of calculated optical absorption spectra in the modulation doping case. The dotted lines represent the results obtained by neglecting the local field effect. The numbers shown in the figure represent N_s. We have introduced a relaxation time given by $\hbar/\tau=5$ meV.

wavefunction which is extended. Correspondingly the local field effect on the transition is negligibly small.

There has been no attempt to observe intersubband optical absorptions, although transitions from the valence band to the conduction band have already been investigated.[6,7] In case of interband transitions, the local field effect as considered here is not important. Instead the conventional exciton effect plays an important role. Its importance has already been observed experimentally,[6] but detailed theoretical study of the exciton effect in the superlattice has not been made yet.

§4. Summary and Conclusion

We have calculated the subband structure of heavily doped GaAs–$Ga_{1-x}Al_xAs$ superlattices taking into account the band bending effect self-consistently. Donor ions have been replaced by uniform positive charges and the calculation has been performed in the Hartree approximation in the two cases, uniform doping and modulation doping. The band bending due to the charge transfer from the $Ga_{1-x}Al_xAs$ to GaAs layers is important in the modulation doping case especially when the wavefunction along the superlattice is localized. Under certain conditions the two lowest subbands turn into levels similar to those in coupled two accumulation layers. Calculated energy separations between them agree with experimental results of Störmer *et al.* although only for a single set of parameters. Future systematic experimental study is highly expected.

The many-body effect such as exchange and correlation has also been studied in the density-functional formulation. It is, however, not so important.

Optical absorption spectra have been calculated. It has been demonstrated that the local field effect is important when the wavefunction is localized and shifts resonance positions to higher energy side considerably.

Acknowledgments

We thank Professor Y. Uemura for valuable discussion and Professor H. Sakaki for discussion on various problems on the superlattice. Numerical calculation has been performed with the aid of HITAC 8800/8700 of the Computer Centre at the University of Tokyo. One of the authors (T.A.) thanks Sakkokai Foundation for the financial support.

References

1) L. L. Chang, L. Esaki and R. Tsu: Appl. Phys. Lett. **24** (1974) 593.
2) L. Esaki and L. L. Chang: Phys. Rev. Lett. **33** (1974) 495.
3) L. L. Chang, H. Sakaki, C. A. Chang and L. Esaki: Phys. Rev. Lett. **38** (1977) 1489.
4) H. Sakaki, L. L. Chang and L. Esaki: *Proc. 14-th Int. Conf. Phys. Semiconductors, Edinburgh, 1978*, ed. B. L. H. Wilson (The Institute of Physics, Bristol, 1978) p. 737.
5) R. Dingle, W. Wiegmann and C. H. Henry: Phys. Rev. Lett. **33** (1974) 1327.
6) R. Dingle, A. C. Gossard and W. Wiegmann: Phys. Rev. Lett. **34** (1975) 1327.
7) R. Tsu, A. Koma and L. Esaki: J. Appl. Phys. **46** (1975) 842.
8) R. Tsu, L. L. Chang, G. A. Sai-Halasz and L. Esaki: Phys. Rev. Lett. **34** (1975) 1509.
9) P. Manuel, G. A. Sai-Halasz, L. L. Chang, C. Chang and L. Esaki: Phys. Rev. Lett. **37** (1976) 1701.
10) G. A. Sai-Halasz, A. Pinczuk, P. Y. Yu and L. Esaki: Solid State Commun. **25** (1978) 381.
11) R. Dingle, H. L. Störmer, A. C. Gossard and W. Wiegmann: Appl. Phys. Lett. **37** (1978) 665.
12) H. L. Störmer, R. Dingle, A. C. Gossard, W. Wiegmann and R. A. Logan: *Proc. 14-th Int. Conf. Phys. Semiconductors, Edinburgh, 1978*, ed. B. L. H. Wilson (The Institute of Physics, Bristol, 1978) p. 557.
13) See, for example, T. Inoshita, K. Nakao and H. Kamimura: J. Phys. Soc. Jpn. **43** (1977) 1237.
14) F. Stern and W. E. Howard: Phys. Rev. **163** (1967) 816.
15) See, for example, T. Ando and Y. Uemura: J. Phys. Soc. Jpn. **31** (1971) 331.
16) P. Hohenberg and W. Kohn: Phys. Rev. **136** (1964) B864.
17) W. Kohn and L. J. Sham: Phys. Rev. **140** (1965) A1133.
18) L. J. Sham and W. Kohn: Phys. Rev. **145** (1966) 561.
19) T. Ando: Phys. Rev. **B13** (1976) 3468.
20) O. Gunnarson and B. I. Lundqvist: Phys. Rev. **B13** (1976) 4274.
21) See, for example, T. Ando: Z. Phys. **B26** (1977) 263.
22) S. L. Adler: Phys. Rev. **126** (1962) 413.
23) N. Wiser: Phys. Rev. **129** (1963) 62.